This article was downloaded by: [Swinburne University of Technology]
On: 07 January 2015, At: 09:05
Publisher: Taylor & Francis
Informa Ltd Registered in England and Wales Registered Number: 1072954 Registered office: Mortimer House, 37-41 Mortimer Street, London W1T 3JH, UK

Journal of Earthquake Engineering
Publication details, including instructions for authors and subscription information:
http://www.tandfonline.com/loi/ueqe20

Shake-Table Tests of Confined-Masonry Rocking Walls with Supplementary Hysteretic Damping

L. A. Toranzo [a] , J. I. Restrepo [b] , J. B. Mander [c] & A. J. Carr [d]
[a] KPFF Consulting Engineers , Los Angeles, California, USA
[b] Department of Structural Engineering , University of California , San Diego, La Jolla, California, USA
[c] Department of Structural Engineering , Texas A&M , College Station, Texas, USA
[d] Department of Civil Engineering , University of Canterbury , Christchurch, New Zealand
Published online: 14 Jul 2009.

To cite this article: L. A. Toranzo , J. I. Restrepo , J. B. Mander & A. J. Carr (2009) Shake-Table Tests of Confined-Masonry Rocking Walls with Supplementary Hysteretic Damping, Journal of Earthquake Engineering, 13:6, 882-898, DOI: 10.1080/13632460802715040

To link to this article: http://dx.doi.org/10.1080/13632460802715040

PLEASE SCROLL DOWN FOR ARTICLE

Taylor & Francis makes every effort to ensure the accuracy of all the information (the “Content”) contained in the publications on our platform. However, Taylor & Francis, our agents, and our licensors make no representations or warranties whatsoever as to the accuracy, completeness, or suitability for any purpose of the Content. Any opinions and views expressed in this publication are the opinions and views of the authors, and are not the views of or endorsed by Taylor & Francis. The accuracy of the Content should not be relied upon and should be independently verified with primary sources of information. Taylor and Francis shall not be liable for any losses, actions, claims, proceedings, demands, costs, expenses, damages, and other liabilities whatsoever or howsoever caused arising directly or indirectly in connection with, in relation to or arising out of the use of the Content.

This article may be used for research, teaching, and private study purposes. Any substantial or systematic reproduction, redistribution, reselling, loan, sub-licensing, systematic supply, or distribution in any form to anyone is expressly forbidden. Terms &

Conditions of access and use can be found at http://www.tandfonline.com/page/terms-and-conditions

Downloaded by [Swinburne University of Technology] at 09:05 07 January 2015

Journal of Earthquake Engineering, 13:882–898, 2009
Copyright © A.S. Elnashai & N.N. Ambraseys
ISSN: 1363-2469 print / 1559-808X online
DOI: 10.1080/13632460802715040

Shake-Table Tests of Confined-Masonry Rocking Walls with Supplementary Hysteretic Damping

L. A. TORANZO[1], J. I. RESTREPO[2], J. B. MANDER[3], and A. J. CARR[4]

[1]KPFF Consulting Engineers, Los Angeles, California, USA
[2]Department of Structural Engineering, University of California, San Diego, La Jolla, California, USA
[3]Department of Structural Engineering, Texas A&M, College Station, Texas, USA
[4]Department of Civil Engineering, University of Canterbury, Christchurch, New Zealand

Downloaded by [Swinburne University of Technology] at 09:05 07 January 2015

A shake-table investigation is conducted on a 40% scale model frame-wall system to validate the concept of rocking walls as primary seismic systems. The rocking wall concept was implemented on confined masonry walls, but the findings can be extended to any rocking wall system. As the inherent damping of this system is low, a pair of supplemental steel hysteretic energy dissipating dampers is used at the base of the wall. It is concluded that with careful detailing, damage is not only eliminated but the structure re-centers itself following a large earthquake.

Keyword Rocking; Rocking Wall; Shake Table Test; Confined Masonry; Performance Based Design

1. Introduction

Recent major earthquakes have caused extensive damage in un-reinforced masonry structures and in structures built incorporating infilled frames [EERI, 2005]. The complex response of structural systems built incorporating traditional materials and methods of construction makes them unusually difficult for use within a performance-based seismic design framework. In many countries there is generally sufficient awareness of the high vulnerability of buildings built with traditional materials and methods of construction, however, the elimination of such methods and materials has economic and social ramifications that can only be understood and measured within the societal context and development of each country. There are, however, a number of techniques and systems that, if incorporated into traditional methods of construction, could significantly reduce the seismic vulnerability of low-rise building construction such as housing and schools. This article investigates one such system for confined masonry walls. The system uses rocking confined-masonry rocking walls that are built with low-cost hysteretic energy-dissipation devices (EDDs). The main aim of using confined-masonry rocking walls is the minimization of structural damage and of residual drifts. With appropriate design and detailing, such systems can be assured to

Received 24 March 2008; accepted 28 December 2008.
Address correspondence to L. A. Toranzo, KPFF Consulting Engineers, 6080 Center Drive, Suite 300, Los Angeles, CA 90045, USA; E-mail: ltoranzo@kpff-la.com

Downloaded by [Swinburne University of Technology] at 09:05 07 January 2015

behave within prescribed drift limits without structural damage. This article presents and discusses the results of a shake-table test program conducted on a 40% scale model of a segment of a prototype three-story school building. The effect of the energy dissipation devices on the dynamic response of the structure is highlighted. Full details of the experimental investigation may be found in Toranzo [2002].

2. Behavioral Mechanisms of Rocking Walls with Supplementary Damping

Rocking walls are detailed such that, under lateral loading, they can rock about their bases. The response of a rocking wall to monotonic lateral loading is nonlinear elastic and its response can be approximated as bilinear. Softening in the response occurs when the overturning moment demand causes decompression in the extreme tensile fiber at the base of the wall, which also marks the onset of rocking.

The ability of rocking to protect structures from earthquakes has been noted as early as the early 1960s [Housner, 1963]. Yet, rocking has not been developed as much as other alternative structural systems, and practical applications of rocking structural systems are scarce [Skinner *et al.*, 1993]. However, the current focus on the performance-based seismic design of buildings has meant that rocking is being explored as an alternative structural solution [Mander and Cheng, 1997; Priestley *et al.*, 1999; Holden *et al.* 2002; Restrepo and Rahman, 2007].

Rocking walls have many positive features from a seismic point of view, the most relevant being their capacity to sustain large lateral displacements without damage and their characteristic re-centering mechanism that prevents any residual deformation. But rocking walls also have negative aspects that need to be addressed if they are to be appropriately used to provide seismic resistance. The most relevant negative features are: low energy dissipation capacity; potential large impact actions; and unpredictable seismic response [Makris and Roussos, 1998].

It can be argued that most of the negative seismic aspects of rocking walls originate from the lack of a reliable source of energy dissipation within the system [Toranzo, 2002]. Hysteretic EDDs placed at the base of rocking walls can provide a dependable source of supplementary energy dissipation, and mitigate the effects caused by impact. A better control of the energy dissipation capacity of the system allows the use of established design techniques for the prediction of the seismic performance of rocking walls [Toranzo, 2002].

Previous research has investigated the seismic response of cantilever rocking wall systems with hysteretic EDDs in the way of mild steel bars anchored at the base of the walls [Holden *et al.*, 2002; Restrepo and Rahman, 2007]. An appealing feature of these devices is their large initial stiffness. However, because they are cast in the concrete it is difficult to establish their health-state following an earthquake; moreover, it would be difficult and expensive to replace such internal devices if severely damaged. Thus, it is considered desirable to adopt external devices for ease of inspection and replacement. Devices similar to the EDD's used in this research are similar, in principle, to those employed in the Union House building in Auckland, New Zealand [Boardman *et al.*, 1983; Skinner *et al.*, 1993].

An external linearly tapered steel cantilever EDD can be designed to meet the energy dissipation requirements in rocking wall systems. The geometry of linearly tapered steel cantilever EDDs must be carefully proportioned in order to provide an initial high-stiffness, provide a stable hysteretic response, avoid fracture or instability before attaining the displacement levels calculated for a "rare" earthquake, and ensure the self-centering response of the walls. Geometrical consideration should also be given in the design to the development of high overstrength due to the gradual participation of axial stiffness as the device is displaced upwards. These EDDs can be placed at the toes of a rocking wall. In this location, the devices dissipate most of the energy through flexure as a result of uplifting and returning to their original positions. An additional appealing feature of these devices is that they can transfer the wall shear force into the foundation, thus reducing the reliance on friction for shear transfer.

3. Description of the Prototype Building and Performance Objectives

The test structure described in this article represents a segment of a typical three-story school/university classroom building found in many parts of South America. The structural system in these buildings is mainly comprised of confined-masonry walls. Confined-masonry is a traditional method of construction that consists of un-reinforced brick masonry panels surrounded by small and lightly reinforced concrete beams and columns [EERI, 2005]. Classroom buildings are rather oblong and have minimum ventilation, light, and space requirements that usually result in a medium to low density of walls. Significant earthquake damage, and the consequential social impact to the community, to these types of buildings has been often reported [Casabone 1994; EERI, 2005]. Figure 1 illustrates the prototype building used to proportion the test specimen.

Design and construction techniques with confined-masonry are such that it is very difficult to establish a failure hierarchy. In buildings that are two to three stories high, it is not uncommon to find shear failures in walls concentrated in a single, often the lowermost, story and that result in a soft-story mechanism. Preventing the development of this mechanism by increasing the design lateral forces is not necessarily possible, nor is the best economic solution.

The concept of controlled rocking as an effective structural system is a possible economic option for buildings built with confined-masonry. Using suitable wall geometry, a strain-design approach in the confining reinforced concrete elements to explicitly prevent shear failure [Crisafulli *et al.*, 2005], and the incorporation of low-cost energy dissipation devices (EDD) can significantly enhance the structural system seismic behavior.

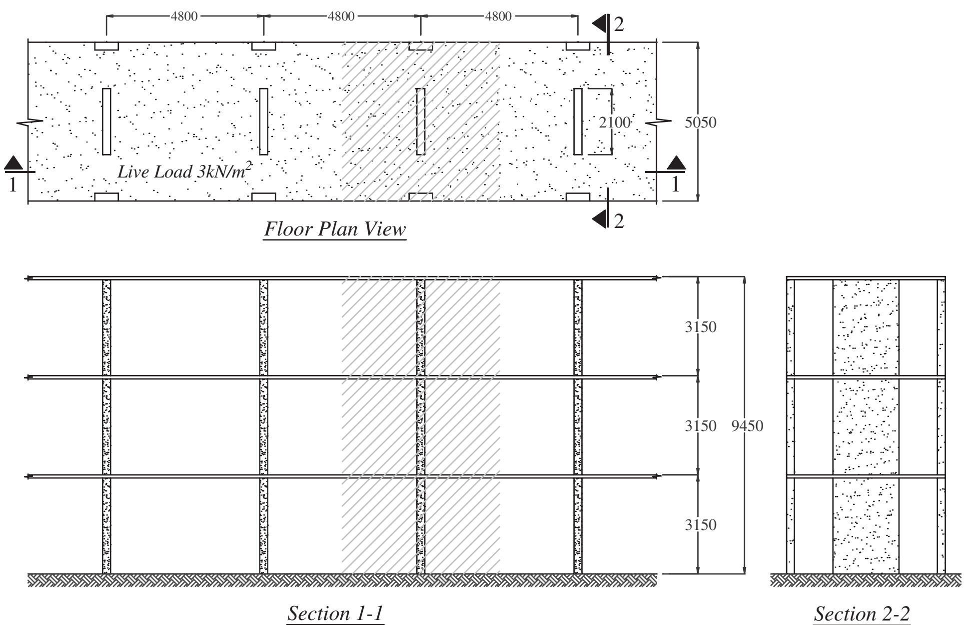

FIGURE 1 Prototype building showing typical slice (hatched) section to be modeled.

Downloaded by [Swinburne University of Technology] at 09:05 07 January 2015

A performance-based design methodology was used in the design of the prototype building system. Four aspects were addressed in the design methodology: (a) prevention of structural damage up to the design earthquake defined by a 475 years return period earthquake; (b) enforcement of a prescribed mechanism, which in this case was the controlled rocking of the walls; (c) control of the extent of lateral drift of the structure during the design earthquake; and (d) prevention of any residual displacement. The rocking wall mechanism was enforced, while the masonry panels were protected using the strain-design approach described previously. The direct displacement based design methodology proposed by Priestley [2000] was adapted for this system in order to control the lateral drift of the structure. A roof drift ratio limit of 1.50% was established as the target drift ratio for the design earthquake.

It appears at first glance that the performance objective chosen to prevent structural damage is excessively stringent. Nevertheless, rocking systems can be easily detailed to prevent any structural damage. Moreover, the combination of capacity and strain-design philosophies can be used to prevent shear failure of the masonry panel up to the maximum credible earthquake.

4. Test Specimen

A 40% scale model, representing a section of the prototype structure, was designed and constructed base on the hatched section shown in Fig. 1. The detailing of the reinforcement in the test structure was intended to ensure that the rocking mechanism chosen in design could develop and be maintained throughout. With the exception of the EDDs, the base of the exterior columns and two specific locations in each of the connecting slabs, all other structural elements were capacity-designed to remain elastic. High rotational capacity-reduced moment capacity zones were detailed deliberately at the slabs and at the base of the columns in specific locations where large rotations were expected to occur. These regions were detailed to ensure reduced influence on the mechanism in the rocking system. In the slabs these regions were formed by grooves. Figure 2 shows the location of the grooves and Fig. 3 shows the probable moment capacities of the yield

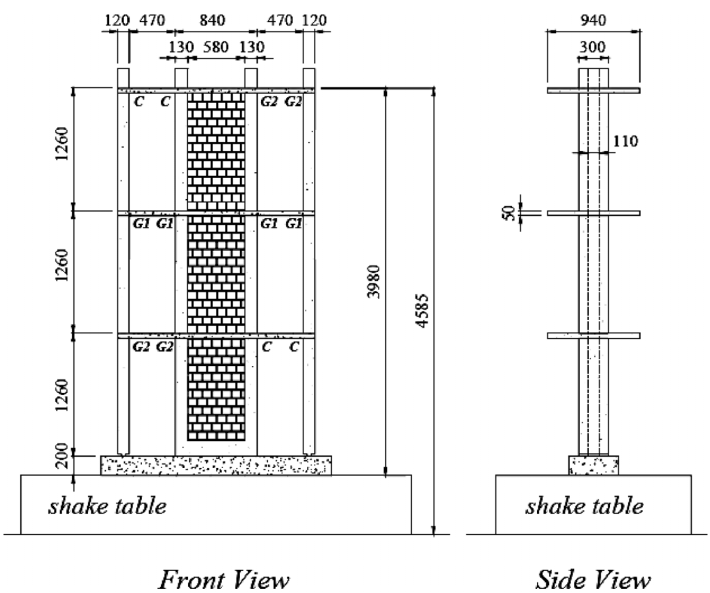

FIGURE 2 General dimensions of the test structure.

Downloaded by [Swinburne University of Technology] at 09:05 07 January 2015

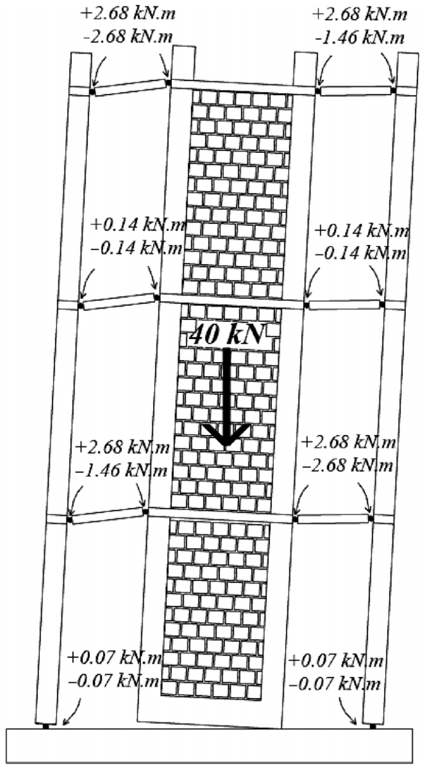

FIGURE 3 Mechanism of non-linear deformation showing flexural capacities.

Downloaded by [Swinburne University of Technology] at 09:05 07 January 2015

lines that could form in these regions. Grooves "G1," with a depth of 10 mm and a width of 20 mm, were built adjacent to the wall and column faces in the first and third floor slabs. The regions without grooves in these slabs are marked as "C" in Fig. 2. Deeper grooves "G2," with a depth of 20 mm and a width of 10 mm, were built adjacent to wall and columns in the second floor. In order to transfer the gravity loads, the reinforcement crossing the grooves was carefully detailed to transfer shear from the section of the slabs spanning between the wall and the exterior columns. This positive longitudinal reinforcement was diagonally bent for this reason to also reduce the flexural stiffness to the slab in the hinge region; see Figs. 4 and 5. The exterior segments of the slabs were reinforced to sustain the adjacent torsion with longitudinal bars (shown in Fig. 5) and closed stirrups (stirrups are not shown in Fig. 5 for clarity). Finally, the base of the exterior columns was detailed to behave as a pin with deep grooves at each side of the middle reinforcement; see Fig. 6.

Large stresses were expected to develop in the toes of the walls at the contact points between the rocking wall and the foundation. To avoid damage, a 10 mm thick steel armor plate was placed in the impacting region of the foundation. For the impacting corners of the rocking wall, a steel armor casing was used to confine the concrete in this region. The arrangement of plates is shown in Fig. 7.

The EDDs transferred their action to the lower corners of the rocking wall. The corners were detailed to transfer these forces to the confining columns using a strain-design approach [Crisafulli *et al.*, 2005]. Steel cylinders were placed at the base of the

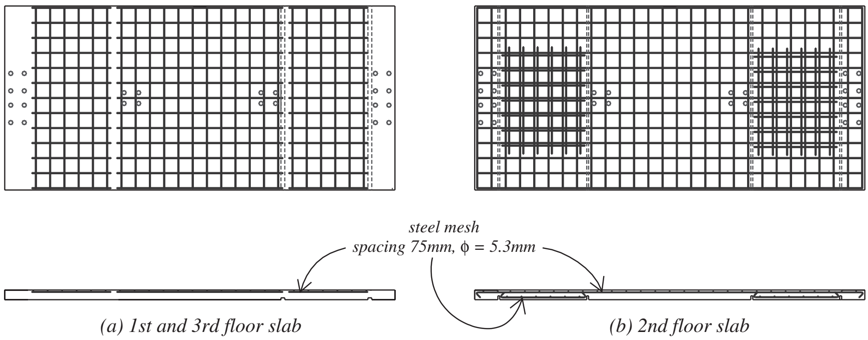

FIGURE 4 Plan and front view of slab showing reinforcing mesh.

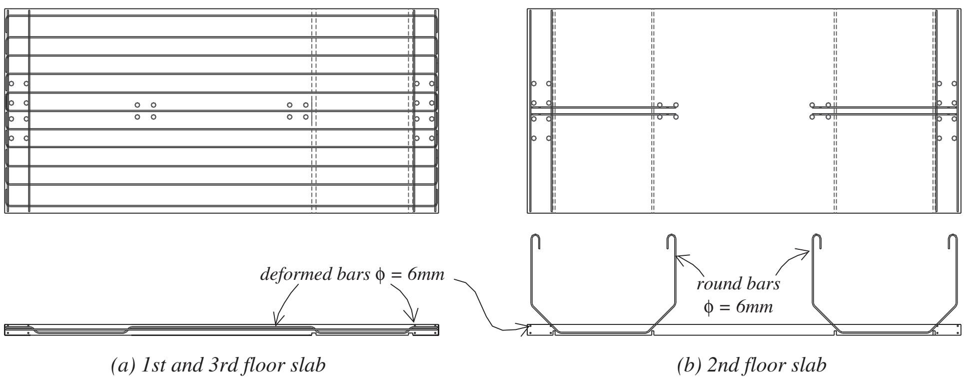

FIGURE 5 Plan and front view of slab showing additional reinforcement.

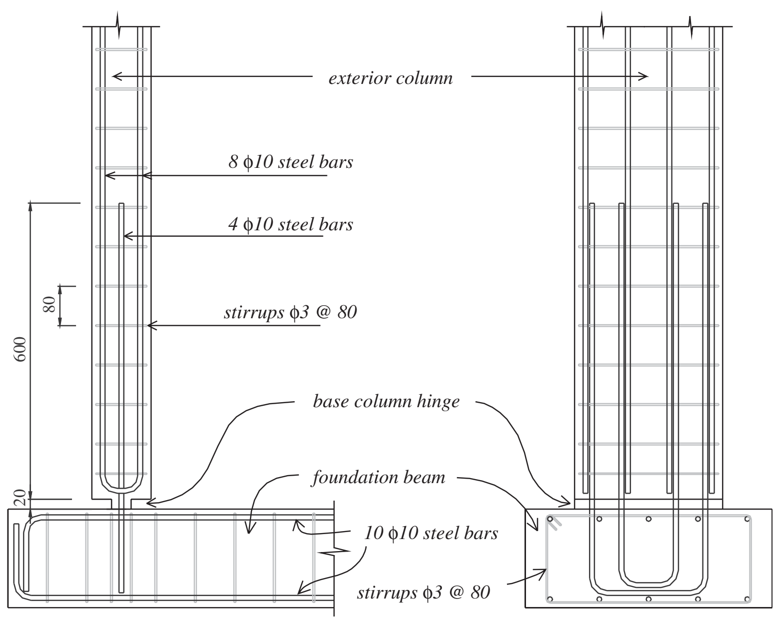

FIGURE 6 Reinforcing detailing at the base of exterior columns.

Downloaded by [Swinburne University of Technology] at 09:05 07 January 2015

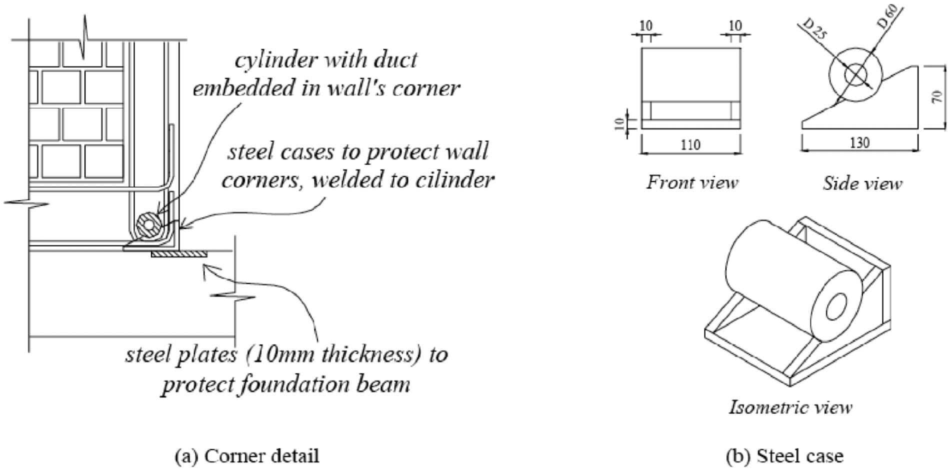

FIGURE 7 Reinforcing detailing at the wall base.

confining columns to receive the force from the EDDs via pins. The tubes, in turn, were surrounded by the longitudinal reinforcement of the columns and the base beam. This detail allowed a direct transfer of forces to the longitudinal reinforcement of the edge columns; see Fig. 7. The other end of the EDDs were fully-fixed to the foundation to allow the EDDs to behave like cantilevers. A bracket was attached to the back end of the EDDs; see Figs. 8 and 9 and these brackets were bolted to a steel plate that was anchored to the foundation. Four EDDs were connected to the base of the wall, two at each side of the wall.

The EDDs were designed to yield at a predetermined vertical force which was established during the design process in order to satisfy energy dissipation requirements, and limit the actions transferred to the masonry panels. The axis of the EDD had a three-degree downward tilt, and a slotted hole which was intended to reduce the participation of axial stiffness as the EDD was displaced upwards (see Fig. 8).

Figure 10 (a) shows the quasi-static test set up for the 40% scale EDD. The devices were subjected to displacement-controlled cyclic loading. The loading protocol consisted of upward displacements to a target level and then a reversal back to the origin, which is expected for these devices in self-centering walls. The devices were subjected to upward displacements of 25 mm, which was in excess of the upward displacement demand of 17 mm

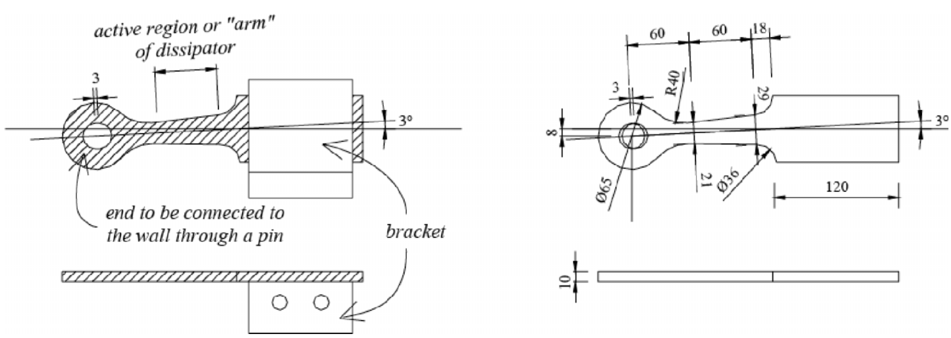

FIGURE 8 Geometry of hysteretic energy dissipation devices.

Downloaded by [Swinburne University of Technology] at 09:05 07 January 2015

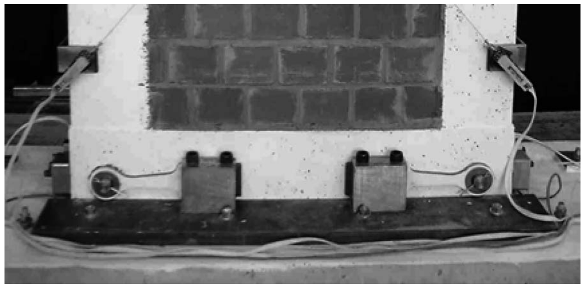

FIGURE 9 View of base of wall with outfitted EDDs.

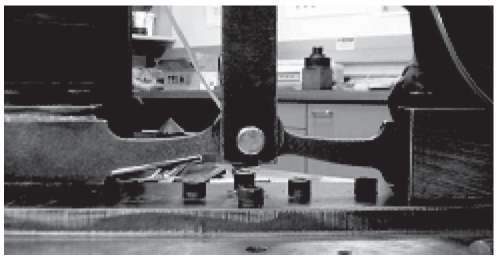

(a) Device at vertical displacement of 25 mm

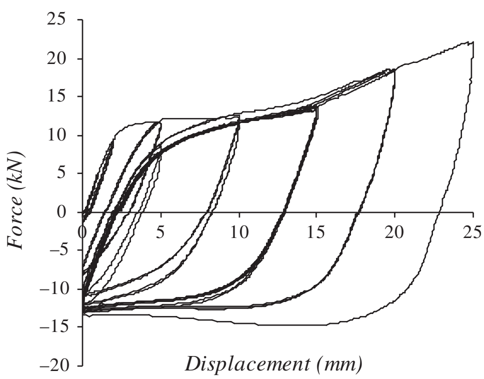

(b) Vertical force–displacement response

FIGURE 10 Hysteretic response characterization of energy dissipation devices.

expected for the device in a ‘‘rare’’ earthquake. The hysteretic response of the device is illustrated in Fig. 10 (b). The gradual participation of the coupled axial stiffness. Strain hardening in the hysteretic response of the devices is particularly clear for upward displacements greater than 15 mm; see Fig. 10 (b).

For the reinforced concrete components, concrete with a specified compressive strength of f’c = 25MPa at 28 days, 75 mm slump and 6 mm maximum aggregate size was used throughout. The slabs and foundation beam were precast whereas all other elements were cast-in-place. Different types of steel reinforcement were used according to necessity and availability in the local market; see Table 1. Locally

Downloaded by [Swinburne University of Technology] at 09:05 07 January 2015

TABLE 1 Nominal characteristics of steel reinforcement

Location in model	Diameter (mm)	Type of bar	Grade (MPa)
Long. Reinforcement in beams and columns	10	deformed	430
Stirrups in beams and columns	4	round	300
Reinforcing mesh in slab	5.3	round	430
Additional reinforcement in slabs	6	deformed	300
Additional reinforcement in slabs	6	round	300

TABLE 2 Mechanical properties of bricks and masonry

Property	Units	#Samples	Average
Clay Bricks			
Compressive strength* (⊥ to bed joint)	MPa	3	27
Tensile strength (// to bed-joint)	MPa	10	1.6
Masonry			
Shear bond strength (brick-mortar)	MPa	6	1.4
Coefficient of friction (brick-mortar)	rad	6	0.57
Ultimate comp. strength* (⊥ to bed-joint)	MPa	8	29
First crack comp. strength* (⊥ to bed-joint)	MPa	8	16

*Uniaxial compression

Downloaded by [Swinburne University of Technology] at 09:05 07 January 2015

manufactured clay solid bricks and ready mixed mortar were used to build the masonry panel. The bricks had an effective area of 78% and were cut in order to achieve the required thickness of the model-masonry-panel. Table 2 presents results of several tests that were conducted to determine the mechanical properties of the bricks and masonry.

Typical construction conditions found in South America [Casabonne, 1994] were reproduced in the construction of the wall. The masonry panel was built first, followed by the construction of confining columns. For logistical reasons, however, the slabs were precast and later placed on top of the wall rather than cast in-situ.

An exterior frame was built to provide lateral stability to the test specimen. The exterior frame allowed the model to have relative displacements of up to 300 mm while providing out-of-plane restrain with minimum friction.

Single axis accelerometers and displacement transducers were deployed at specific locations in the system to monitor accelerations, relative displacements, and shear strains. Full details of the instrumentation are given by Toranzo [2002]. The experiments were performed on the displacement-controlled unidirectional shake-table at the Department of Civil Engineering at the University of Canterbury, New Zealand.

5. Input Ground Motions

Sixty dynamic tests were run. However, some of them are only marginally relevant, as they were used to observe the fidelity of the signal rather than to observe the seismic performance of the model. The first runs (1–3, 5–8, and 10 to 11) were mainly used to determine the natural periods of the structure. Runs 12–54 were intended to reproduce the seismic demand at the different design levels. Some runs in between, however, were only conducted as trials to check the instrumentation. These trial runs were scaled down to produce very low levels of demand. Thanks to the large number of dynamic tests it was possible to test the system under different conditions. Two sets of dissipators in runs 46–58. The program concluded with runs 55–60, where the structure was subjected to sine-type impulses to observe its free-oscillation response with and without EDDs. The complete schedule of tests is listed in Table 3. Selected tests whose results will be used in this paper to illustrate the most important findings of this research have been highlighted in Table 3 and are referenced in the sections below. A comprehensive description of all results can be found in Toranzo [2002].

Five historical ground motions were chosen and their amplitudes scaled to induce demand-levels equivalent to the design spectrum, for performance-objectives that

TABLE 3 Summary of runs

Test	Description	Scale factor(1)	Expected peak acceleration (g)
Rocking wall with first set of EDD's			
Run 01	Impact at 3rd floor	–	–
Run 02	Impact at 2nd floor	–	–
Run 03	Impact at 1 st floor	–	–
Run 04	translation +/−50mm	–	–
Run 05	White Noise 1	0.10	0.01
Run 06	White Noise 1	0.50	0.03
Run 07	White Noise 2	0.50	0.03
Run 08	White Noise 2	1.00	0.05
Run 09	Taft-a	0.50	0.09
Run 10	Impact at 1st floor	–	–
Run 11	Impact at 1st floor	–	–
Run 12	Taft-b	0.50	0.08
Run 13	Saticoy	0.10	0.05
Run 14	Saticoy	0.25	0.11
Run 15	Taft-a	0.10	0.02
Run 16	Taft-a	0.50	0.10
Run 17	Taft-b	0.10	0.02
Run 18	Taft-b	0.50	0.08
Run 19	Saticoy	0.25	0.11
Run 20	El Centro	0.10	0.04
Run 21	**El Centro**	**0.56**	**0.20**
Run 22	Taft-a	0.10	0.02
Run 23	Taft-a	1.13	0.20
Run 24	El Centro	0.84	0.30
Run 25	Taft-a	1.69	0.30
Run 26	El Centro	1.12	0.40
Run 27	Taft-a	2.26	0.40
Run 28	Sylmar	0.50	0.40
Run 29	El Centro	1.40	0.50

(*Continued*)

Downloaded by [Swinburne University of Technology] at 09:05 07 January 2015

Downloaded by [Swinburne University of Technology] at 09:05 07 January 2015

TABLE 3 (*Continued*)

Test	Description	Scale factor[1]	Expected peak acceleration (g)
Run 30	Taft-a	2.83	0.50
Run 31	Sylmar	0.63	0.50
Run 32	Taft-a	0.10	0.02
Run 33	El Centro	0.10	0.04
Run 34	El Centro	0.56	0.20
Run 35	Taft-a	1.13	0.20
Rocking wall with second set of EDD's			
Run 36	El Centro	0.10	0.04
Run 37	Taft-a	0.10	0.02
Run 38	**El Centro**	**0.56**	**0.20**
Run 39	Taft-a	1.13	0.20
Run 40	**El Centro**	**1.40**	**0.50**
Run 41	Taft-a	2.83	0.50
Run 42	Sylmar	0.63	0.50
Run 43	Sylmar	1.00	0.80
Run 44	Sylmar	1.00	0.80
Run 45	Sylmar	1.25	1.00
Rocking wall without EDD's			
Run 46	El Centro	0.10	0.04
Run 47	Taft-a	0.10	0.02
Run 48	El Centro	0.56	0.20
Run 49	**El Centro**	**0.56**	**0.20**
Run 50	Taft-a	1.13	0.20
Run 51	**El Centro**	**1.40**	**0.50**
Run 52	Taft-a	2.83	0.50
Run 53	Sylmar	0.63	0.50
Run 54	Sylmar	1.00	0.80
Run 55	Sine Pulse +/−2mm 2Hz	–	–
Run 56	Sine Pulse +/−10mm 2Hz	–	–
Run 57	Sine Pulse +/−10mm 2Hz	–	–
Run 58	**Sine Pulse +/−40mm 5Hz**	–	–
Rocking wall with second set of EDD's back in position			
Run 59	**Sine Pulse +/−40mm 5Hz**	–	–
Run 60	Sine Pulse +/−80mm 5Hz	–	–

[1]This refers to the amplitude scale factor applied to the record to obtain the target performance level and not that required for similitude.

corresponded to return periods of 43, 75, 475, and 970 years. Both amplitude and time were modified by the appropriate similitude ratios.

There were difficulties in the reproduction of the ground motions by the shake-table. Acceptable agreement between command and feedback motions was observed in the period band between 0.15–0.55 s but lacked fidelity elsewhere, particularly, in the period band of 0–0.15 s where spectral accelerations consistently exceeded those of the command signal. Details on this deficiency are discussed by Rodriguez *et al.* [2005].

Downloaded by [Swinburne University of Technology] at 09:05 07 January 2015

6. Experimental Results

The system tested performed excellently throughout the experimental program. At the end of the test program, only limited damage was observed in the slabs, no residual displacements were observed, the structure retained its lateral design capacity, and the vertical load capacity of the slabs was preserved throughout the test program. As expected by design, the wall and, in particular, the impacting regions remained intact. Careful inspection of the EDDs also showed no damage. The tests also validated the expected ability of the dissipators to provide the system with significant supplemental energy dissipation capacity. Select test results of the experimental program are described below.

6.1. Natural Periods

The natural period of the system was obtained from the free vibration segment of the time history sequence at the end of each run, when rocking had subsided. In the initial runs a natural period of 0.14 s was observed. As expected, the natural period lengthened mainly as a result of the gradual development of cracking and then propagation of yield lines in the slabs. At the end of Run 40, when significant propagation of yield lines had occurred in the slabs, the observed natural period of the system had lengthened to 0.22 s.

6.2. Residual Displacements

The roof displacement observed in Run 40 is shown in Fig. 11 along with the base uplift of the rocking wall. This was one of the most demanding ground motions imposed on the structure and resulted in a peak wall drift (measured at the roof level) of 2.0%; no residual displacement was observed when all motion subsided. Complete recentering was observed throughout the entire experimental program.

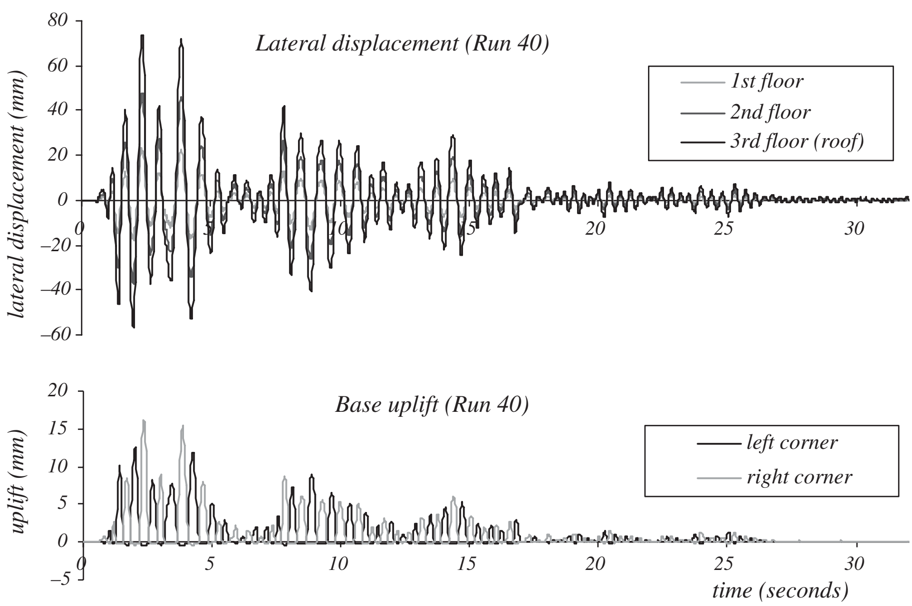

FIGURE 11 Recorded lateral displacements and wall uplift time-histories.

6.3. Hysteretic Response

To assess the overall effect of the supplementary hysteretic damping to the seismic response, this section describes the system's response for two levels of excitation, and compares the response of the system with and without EDDs. Tests were carried out to observe the system's dynamic response at four levels of excitation. Figure 12 shows the hysteretic performance obtained during Runs 38, 40, 49, and 51. EDDs were incorporated into the system for performing Runs 38 and 40 and removed in Runs 49 and 51. As detailed in Table 3, Run 38 (with EDDs) and Run 49 (without EDDs) consisted of identical input ground motions that represented earthquakes with a 72-year return period. Similarly, the input ground motions of Run 40 (with EDDs) and Run 51 (without EDDs) were identical and represented earthquakes with a 970-year return period. When comparing the system's response in Runs 38 and 49 and in Runs 40 and 51, it is evident that the removal of the EDDs, respectively, resulted in 50% and 33% greater lateral displacement demands.

6.4. Lateral Force Capacity

The theoretical lateral force capacity was evaluated for two possible scenarios, each considering the mechanism of nonlinear deformation shown in Fig. 6, as well as accounting for the EDDs, if present. The first scenario accounted for the moment capacities of the slabs, as shown in Fig. 6. The second scenario ignored the contribution of the slabs altogether. The justification for the second scenario was the substantial stiffness degradation expected in the slabs after the formation of yield lines. The location of the lateral force was calculated assuming a first mode of response and a linear mode shape. The lateral force capacity calculated for the first and second scenarios are shown in Fig. 12 as HsI and Hn, respectively.

The contribution of the slabs to the system's response can be observed by comparing the hysteretic responses of Runs 21 and 38; see Fig. 13. The input ground motion for

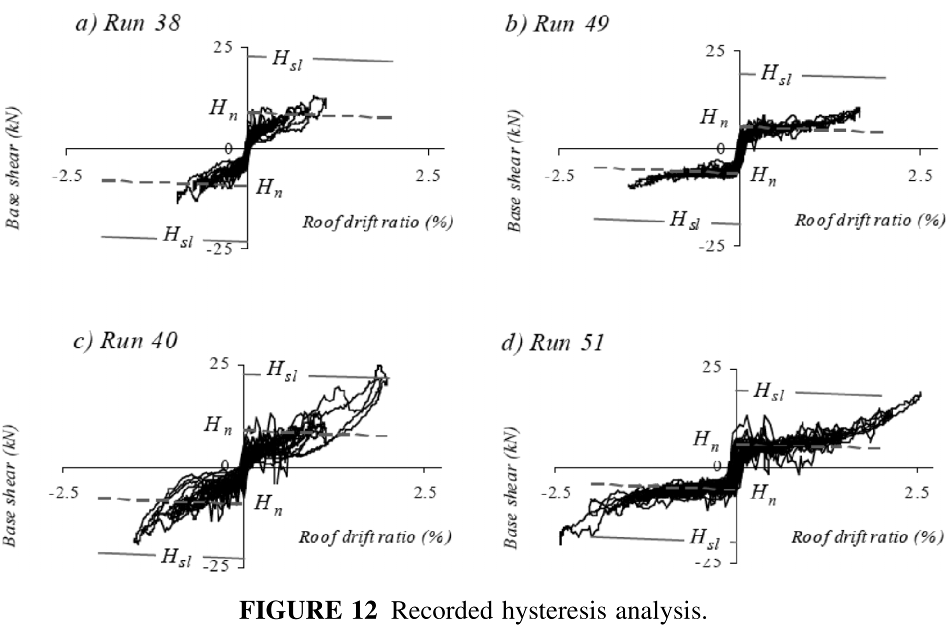

FIGURE 12 Recorded hysteresis analysis.

Downloaded by [Swinburne University of Technology] at 09:05 07 January 2015

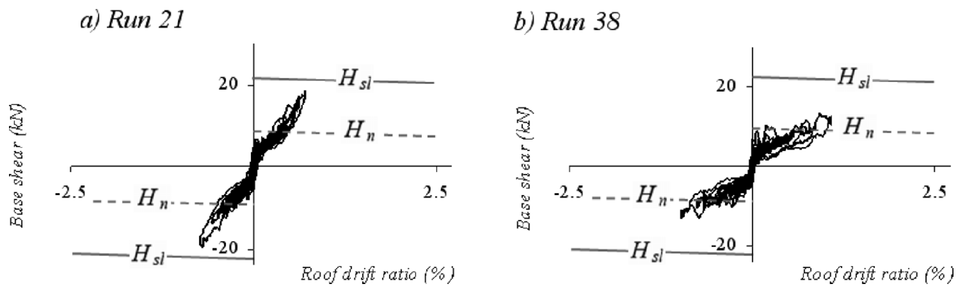

FIGURE 13 Influence of slab in the system hysteretic response.

these two runs was identical. The only difference was that, prior to Run 21, the system had yet to experience significant Roof Drift Ratio (RDR) demands. During Run 21, the system underwent 0.74% RDR. Yield lines began to spread in the slabs during this run and, thus, the capacity of the yield lines contributed significantly to the lateral force resistance. By Run 38, degradation of the slab stiffness had occurred and the slab contribution to the lateral force resistance was rather limited.

6.5. Free-vibration Response

The effect that the EDDs had on the system response was also observed in the free-vibration response of Runs 58 and 59 when the system was excited with a pulse. Figure 14 plots the roof horizontal acceleration in Runs 58 and 59. A new set of EDDs was outfitted prior to Run 59 while Run 58 was performed without EDDs. A comparison of the system's response to these runs clearly shows the strong dampening effect caused by the presence of the EDDs. The system response in Run 58 was characterized by a

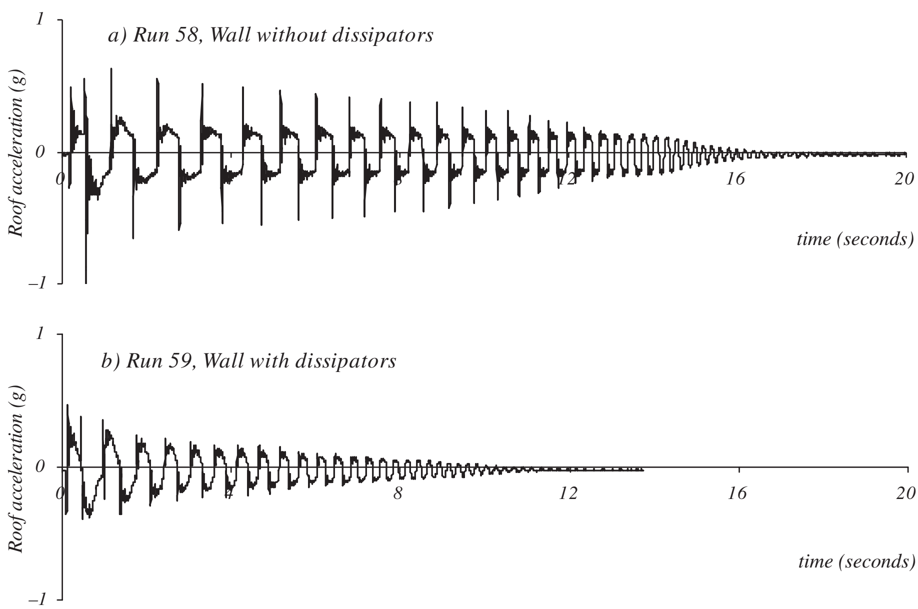

FIGURE 14 System-free vibration responses.

Downloaded by [Swinburne University of Technology] at 09:05 07 January 2015

predominantly low-frequency near-square wave with a high-frequency spike that resulted from the impacting of the wall toes into the foundation; see Fig. 14 (a). The presence of the EDDs softened the low-frequency wave and dramatically dampened out the high-frequency spike; see Fig. 14 (b).

6.6. Equivalent Viscous Damping (EVD)

EVD values were obtained from the decay of the roof lateral displacement time-history response between consecutive cycles in Runs 58 and 59. In Run 58, the EVD values obtained chiefly reflect components of intrinsic and radiation damping, while in Run 59 they account for energy dissipated by the EDDs. At this point in the experimental program, the slabs had lost stiffness and only contributed to energy dissipation at large RDRs. Figure 15 shows that the system, when stripped of the EDDs, was only lightly damped; EVD values ranged between 1.6 and 2.8% for RDRs less than 1.2%. EVD values increased at larger drifts mainly because of the gradual participation of the slabs in the response. At 2.3% RDR the system reached an EVD value of 4.9%. The incorporation of the EDDs resulted in a gradual increase of EVD values from 0.3% RDR, which was approximately the drift level at the onset of yielding of the EDDs. At 1.9% RDR an EVD of 14% was obtained for the system.

6.7. Extent of Damage

After 60 test runs the only damage to the structure was observed in some of the slabs, and was mainly restricted to those slabs that had a shallow groove, or did not have the groove along the hinge (Fig. 16). The damage, however, was limited to the concrete within the hinge regions, without compromising the slab gravity-load carrying capacity. The rest of the structure, including the foundation beam, did not show any sign of damage. Apart from their expected residual stress, the EDDs were also in excellent condition.

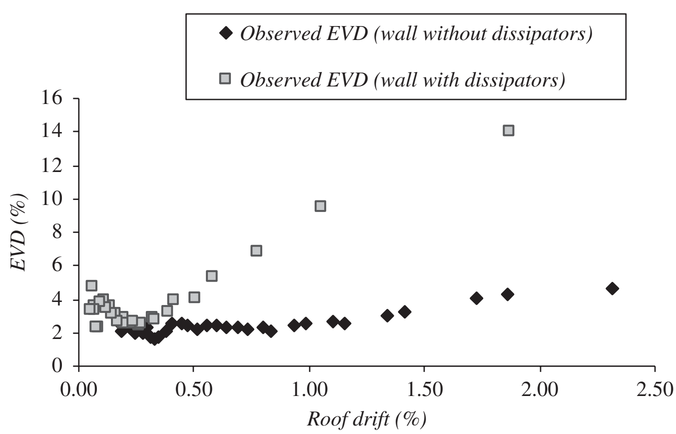

FIGURE 15 System equivalent viscous damping.

Downloaded by [Swinburne University of Technology] at 09:05 07 January 2015

Downloaded by [Swinburne University of Technology] at 09:05 07 January 2015

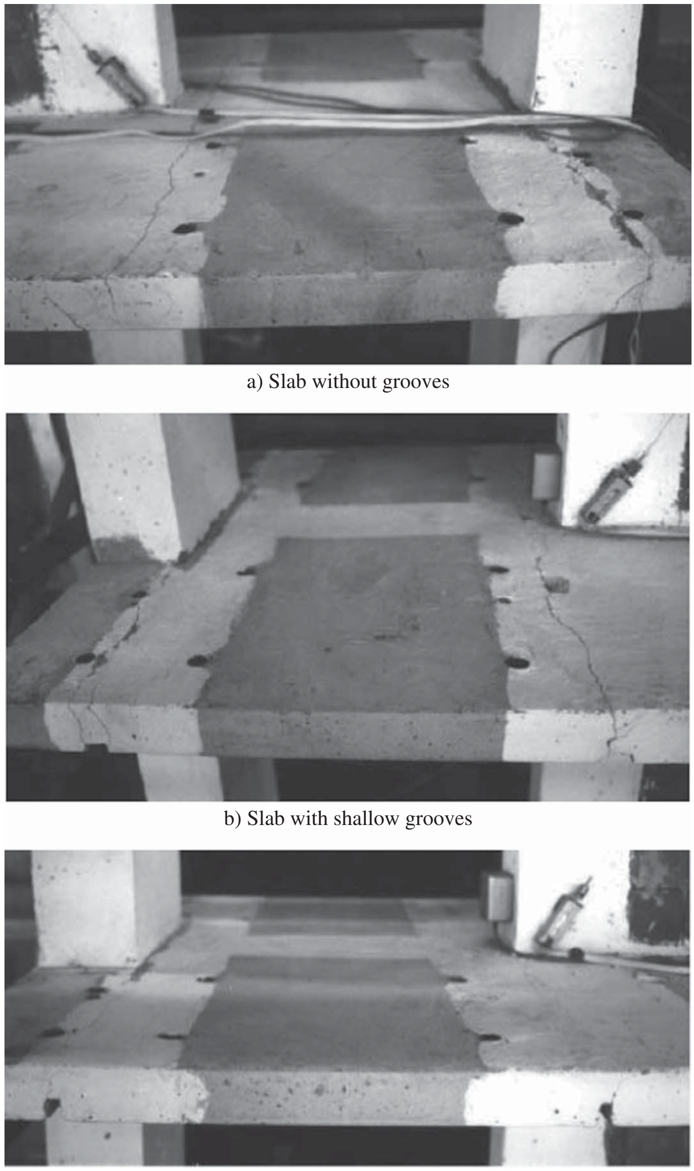

a) Slab without grooves

b) Slab with shallow grooves

c) Slab with deep grooves

FIGURE 16 Extent of damage in slabs at the end of test program.

7. Conclusions

Based on the experimental study presented herein, the following principal conclusions are drawn.

1. The 40% scale model confined brick masonry system performed well under seismic excitation when tested on the shaking table. The test system was subjected to 60 input ground motions and reached a maximum roof drift ratio of 2.5% without discernible damage. The reason for this good performance is attributed to a confined masonry rocking wall.

2. In order for the rocking wall details to work well, it is desirable to provide armoring at the rocking interface. This mitigates crushing of the concrete and bricks under the high point forces that form when the wall rocks back and forth from heel to toe. Armoring using steel plate was demonstrated to be a viable solution.
3. It is desirable, although not essential, to introduce some form of supplemental damping into the system. This is because rocking systems suffer from low inherent damping. With no supplemental dampers present, at low amplitude drifts damping was observed to be less than 3% of critical in the experiments. With the supplemental steel hysteretic dampers present, the equivalent damping ratio increased to 14%. Without dampers, lateral displacement demands increased between 33 and 50%.
4. A major advantage of rocking systems is that they are self-centering. In the present experiments, no residual deformations were observed.

Acknowledgments

The Ministry of Foreign Affairs of New Zealand provided a Doctoral scholarship for the first author. The authors thank Dr. John Pickering, Kevin Wines, John Maley, and Stuart Toase from the University of Canterbury for the support provided in the successful completion of this work.

References

Boardman, P. R., Wood, B. J., and Carr, A. J. [1983] "Union House-a cross-braced structure with energy EDDs," *Bulletin of the New Zealand Society for Earthquake Engineering* **16**(2), 83–97.

Casabone, C. [1994] "General description of systems and construction practices," Masonry in the Americas, American Concrete Institute, Paper SP 147–2.

Crisafulli, F. J., Carr, A. J., and Park, R. [2005] "Experimental response of framed masonry structures designed with new reinforcing details," *Bulletin of the New Zealand Society for Earthquake Engineering* **38**(1), 19–32.

EERI [2005] World housing project. http://www.world-housing.net/

Holden, T., Restrepo, J. I., and Mander, J. B. [2002] "Seismic performance of precast reinforced and prestressed concrete walls," *Journal of Structural Engineering, ASCE* **129**(3), 286–296.

Housner, G. W. [1963] "The behavior of inverted pendulum structures during earthquakes," *Bulletin of the Seismological Society of America*, **53**(2), 403–417.

Makris, N. Roussos, Y. [1998] "Rocking response and overturning of equipment under horizontal-type pulses," Report No PEER-98/05, University of California, Berkeley.

Mander, J. B. and Cheng, C. T. [1997] "Seismic resistance of bridge piers based on damage avoidance design," Technical Report NCEER-97-0014 (National Center for Earthquake Engineering Research), State University of New York, Buffalo, December 10.

Priestley, M. J. N., Sritharan, S., Conley, J. R., and Pampanin, S. [1999] "Preliminary results and conclusions from the PRESSS five-story precast concrete test building," *PCI Journal* **44**(6), 42–67.

Priestley, M. J. N. [2000] "Performance-based seismic design," *Bulletin of the New Zealand Society for Earthquake Engineering* **33**(3), 325–347.

Restrepo, J. I. and Rahman, A. [2007] "Seismic performance of self-centering structural walls incorporating energy dissipators," *Journal of Structural Engineering, ASCE* **133**(11), 1560–1570.

Rodriguez, M. E., Restrepo J. I., and Blandon, J. J. [2005] "Shaking table tests of a four-story miniature steel building-model validation," *Earthquake Spectra* **22**(3), 755–780.

Skinner, R. J., Robinson, W. H., and McVerry, G. H. [1993] *An Introduction to Seismic Isolation*. Wiley, New York.

Toranzo, L. [2002] "The use of rocking walls in confined masonry structures: a performance-based approach," PhD Thesis, Department of Civil Engineering, University of Canterbury, New Zealand.

Downloaded by [Swinburne University of Technology] at 09:05 07 January 2015